One-step synthesis and characterisation of LuAG nanoparticles via solvothermal route

Lin Xing ✉, *Conghui Wang, Xiujie Wang, Xingxing Ding*

College of Science, Zhongyuan University of Technology, Zhengzhou 450007, People's Republic of China
✉ *E-mail: hahaxinglin@sina.com*

Published in Micro & Nano Letters; Received on 28th May 2017; Revised on 30th August 2017; Accepted on 5th December 2017

Lutetium aluminium garnet ($Lu_3Al_5O_{12}$, LuAG) nanoparticles were well prepared via a facile and low temperature one-step solvothermal route using aluminium nitrate and lutetium nitrate as raw materials and ethylenediamine (en) solution as the reaction medium. Here, en was employed both as the chelating agent and structure-directing agent. Influences of the reaction medium, temperature, time and dispersant on the synthesis of crystalline LuAG nanoparticles were investigated. Characterisation of LuAG nanoparticles was performed using X-ray diffraction, Fourier transform infrared, transmission electron microscopy and selected area electron diffraction. Optimum synthesis conditions of single-phase LuAG nanoparticles have been determined. The addition of citric acid as a dispersant can effectively decrease the particle size and increase dispersion of crystalline LuAG nanoparticles.

1. Introduction: Lutetium aluminium garnet (LuAG), similar to yttrium aluminium garnet ($Y_3Al_5O_{12}$, YAG), is considered to be a promising scintillator and laser host material [1–3]. The garnet lattice is cubic with eight formula units in each unit cell and symmetry group Ia3d [4]. Currently, doped-LuAG single crystals are mainly used in practical applications. However, their growth processes are time-consuming and arduous, and also difficult to obtain large-size single crystals, leading to high production cost and limited applications [5]. As an alternative, the preparation of transparent high-density polycrystalline ceramic is a good solution. To achieve this goal, the key step is the preparation of LuAG nanoparticles [1].

Many routes have been employed to prepare LuAG nanoparticles, such as solid-state reaction method [6, 7], co-precipitation method [8, 9], sol-gel method [10, 11], and solvothermal method [2, 5, 12]. In these techniques, the solid-state reaction route is easy, however, the reaction is often incomplete and some reactants stay in the final product. While high purity nanoparticles with uniform components and ultrafine grains can be obtained via other chemical routes, their preparation processes are complex and usually require two or three steps to complete the growth of crystallites. Therefore, it is necessary to find a simple method to synthesise LuAG nanoparticles.

In this work, LuAG nanoparticles were well prepared via a facile one-step solvothermal process. The influences of reaction medium, temperature, time and dispersant on LuAG nanoparticles were investigated and the best conditions for the synthesis of LuAG nanoparticles were presented.

2. Experimental: Lutetium nitrate (99.9%) and aluminium nitrate (analytical grade) were uniformly mixed in a mortar with Lu^{3+}/Al^{3+} mole ratio of 3:5. If citric acid (analytical grade) was used as a dispersant, a certain amount of citric acid would be added into the mixtures. The mixtures were then added into ethylenediamine (en, analytical grade)–water followed by vigorous stirring to form a uniformly dispersed suspension. Here, R was the value of en:water volume ratio (1:1, 2:1, 3:1 and 1:0). Thereafter, the resulting suspension was sealed in a Teflon-lined stainless steel autoclave, heated up to 180–220°C (heating rate: 1°C/min), kept at this temperature for 3–10 h, and then cooled down naturally to room temperature. The as-prepared precipitants were collected by centrifugation and washed repeatedly using deionised water and anhydrous ethanol. Finally, the powders were collected by drying the precipitates in a vacuum oven at 80°C for 2 h in air.

The structural analysis of the products was performed on a Shimadzu-XRD6000 X-ray diffractometer (XRD) using CuKα as the source. The morphology, average size and crystallinity were examined using a Jeol-JEM200CX transmission electron microscope (TEM). The composition of different reaction products was determined using a Nicolet-NEXUS870 Fourier transform infrared (FTIR) spectrometer with a 4 cm^{-1} resolution in the range of 400–4000 cm^{-1} by the familiar KBr disc method.

3. Results and discussion

3.1. Influence of reaction medium: Fig. 1 displays XRD patterns of the particles prepared at 220°C for 10 h with different en:water volume ratios R, as well as the standard XRD patterns of these phases, such as LuAG (73–1368), LuOOH (72–0928) and γ-AlOOH (83–2384). The structural transformation in these powders can thus be examined. When R = 1:1 (Fig. 1*a*), the as-synthesised powders are identified to be LuOOH and γ-AlOOH, not LuAG. When R = 2:1 (Fig. 1*b*), LuAG characteristic peaks start to form. Meanwhile, the diffraction peak intensities of LuOOH and γ-AlOOH diminish. Thus, it can be inferred from this point that three species (LuOOH, γ-AlOOH and LuAG) exist together. With further increase of R up to 3:1 (Fig. 1*c*), though all three phases coexist, it can be seen that the LuAG phase is dominant in the XRD pattern. When R = 1:0 (Fig. 1*d*), namely, the solvent is only en, it can be found that LuAG is the sole phase.

During the above solvothermal reaction process, en is believed to act as the solvent, chelating agent, and structure-directing agent, which is vital in preparing the crystalline LuAG nanoparticles. Thus, the following mechanism of reaction for different ratios R is proposed. As is well known, en is strongly alkaline and completely soluble in water. Since its small stepwise equilibrium constants (or dissociation constants), the majority of en are in molecular form. Considering the dissolution–crystallisation or dissolution–precipitation processes in solvothermal/hydrothermal preparation, when R = 1:1, polymolecular ring-like hydroxides and en complexes, such as $[Lu_x(OH)_{3x}]$, $[Al_y(OH)_{3y}]$, $[Lu_x(OH)_{3x}{\cdot}(en)_z]$ and $[Al_y(OH)_{3y}{\cdot}(en)_z]$ [2, 13], may be produced in the weak alkaline solution. As the reaction temperature increases, the products start to dehydrate and decompose the organic components and then directly crystallise (precipitate) to transform LuOOH and γ-AlOOH phases. When R is between 2:1 and 3:1, that is, increasing en

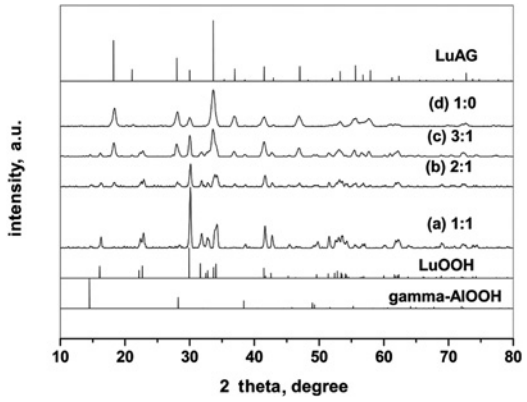

Fig. 1 *XRD patterns of the particles prepared at 220°C for 10 h with different en:water volume ratios R and the standard XRD patterns of γ-AlOOH (83–2384), LuOOH (72–0928) and LuAG (73–1368)*

concentration, the alkalinity of the solution is gradually enhanced. In addition to the above hydroxides and en complexes, new complexes $[Lu_mAl_nO_x(OH)_y{\cdot}(en)_z]$ may appear and resemble the growth units of LuAG lattice [2, 13]. With the increase of reaction temperature, the products dehydrate and decompose the organic components to produce LuOOH, γ-AlOOH and LuAG. Furthermore, the greater the concentration of en, the stronger its complexing ability, the more LuAG crystallites. When $R = 1{:}0$, i.e. only en is used as solvent, single complex $[Lu_mAl_nO_x(OH)_y{\cdot}(en)_z]$ should be produced because of the strong complexing ability of en and pure LuAG is obtained. Therefore, it can be concluded that the presence of en is conducive to the evolution of the LuAG phase and can significantly inhibit the growth of LuOOH and γ-AlOOH phases whereas the addition of water shows the opposite effect.

3.2. Influence of reaction temperature: Fig. 2 shows the XRD patterns of as-synthesised particles in en solution for 10 h with different reaction temperatures (180–220°C). As can be seen, the products are amorphous at 180°C (Fig. 2*a*), and a small amount of the LuAG crystalline phase occurs with the reaction temperature increasing to 190°C (Fig. 2*b*). When the temperature is higher than 200°C, the LuAG crystalline phase has been fully converted from the amorphous state (Figs. 2*c*–*e*). Furthermore, a general trend is that as the reaction temperature increases, the intensities of the diffraction peaks gradually increase (Figs. 2*b*–*d*) and then remain almost unchanged (Figs. 2*d* and *e*).

Fig. 3 shows the FTIR patterns of as-synthesised particles in en solution for 10 h with different reaction temperatures (180–220°C). It can be seen that all the products give FTIR spectra of essentially the same shape in the range of

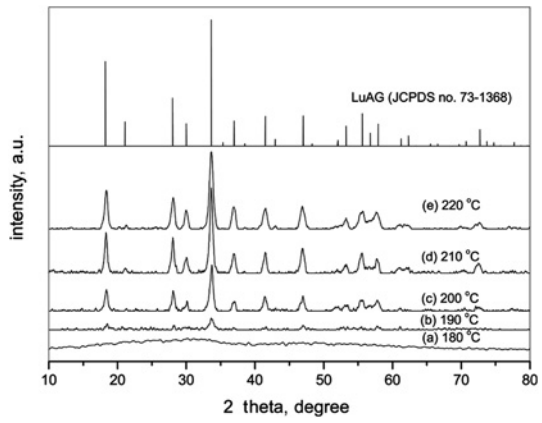

Fig. 2 *XRD patterns of as-prepared particles in en solution for 10 h with different reaction temperatures*

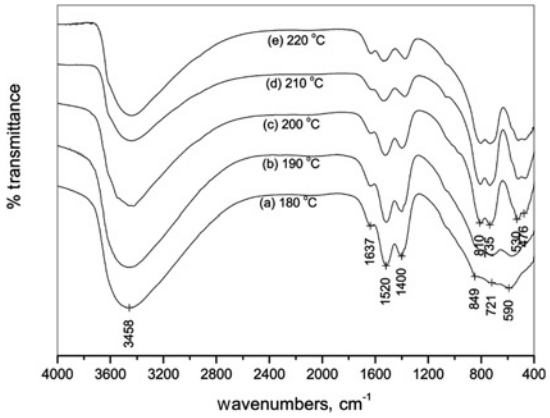

Fig. 3 *FTIR patterns of as-prepared particles in en solution for 10 h with different reaction temperatures*

4000–1200 cm^{-1}. The absorption bands at 3458 and 1637 cm^{-1} are ascribed to O–H stretching and bending vibrations of physically adsorbed H_2O on the sample surface, respectively. The bands at 1520 and 1400 cm^{-1} are attributed to C–H deformation vibrations [14]. However, by comparing the FTIR spectra in the fingerprint region (900–400 cm^{-1}), it is found that the reaction temperatures have a strong influence on the FTIR spectra. Combined with the results of XRD in Fig. 2, it can be concluded that the split absorption bands in Figs. 3*c*–*e* are attributed to M–O bond vibrations because of the formation of the LuAG crystalline phase at reaction temperatures >200°C. The weak peak at 849 cm^{-1} (Fig. 3*a*) may be ascribed to N–O bond vibration [15] due to the amorphous product produced at 180°C. As can be seen from Fig. 3*b*, when the reaction temperature is increased to 190°C, a new band at 810 cm^{-1} shows up in the absorption spectrum. This band stays at higher temperatures (Figs. 3*c*–*e*). Thus, we infer that the LuAG crystalline phase and amorphous phase coexist under this condition. In short, the FTIR results are consistent with XRD analysis in Fig. 2.

Fig. 4 reveals TEM micrographs and selected area electron diffraction (SAED) patterns of as-synthesised particles in en solution

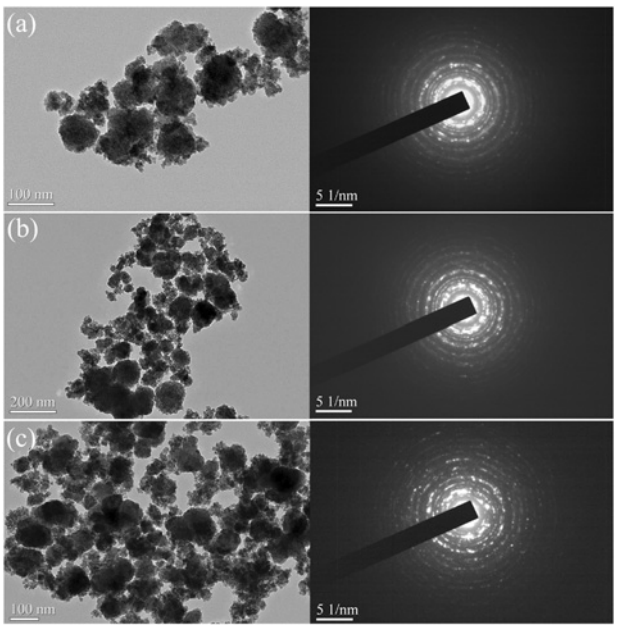

Fig. 4 *TEM micrographs and SAED patterns of as-prepared particles in en solution for 10 h with different reaction temperatures*
a 200°C
b 210°C
c 220°C

doi: 10.1049/mnl.2017.0316

for 10 h with different reaction temperatures (200–220°C). As can be seen clearly from these SAED patterns, the as-synthesised products are well-crystalline. TEM micrographs show that the as-obtained nanoparticles have almost spherical structural morphology with a particle size of around 100 nm. This proves that the particle size and morphology are almost not affected at a reaction temperatures >200°C. Combined with the results obtained from XRD patterns (Fig. 2) and FTIR spectra (Fig. 3), it can be concluded that nanoparticles observed in Fig. 4 are single phase crystalline LuAG.

3.3. Influence of reaction time: Fig. 5 reveals that XRD patterns of as-synthesised particles in en solution at 220°C using different reaction times (3–10 h). It can be found that the pure LuAG powders can be obtained if the retaining time is 3 h or more. Moreover, the diffraction peak intensities and positions do not change significantly with the prolongation of reaction time (Figs. 5*b–d*).

Fig. 6 presents TEM micrographs and SAED patterns of as-synthesised particles in en solution at 220°C using different reaction times (3–10 h). It is clear that a common characteristic of the nanoparticles is their near-spherical shape. All the samples reveal to be well-crystallised and also slightly agglomerated. With prolonging the reaction time, the grain size gradually grows up (Figs. 6*a–c*) and finally stabilises at about 100 nm (Fig. 6*d*). Combined with the above XRD analysis (Fig. 5), it is evident that the products are pure-phase LuAG nanoparticles. In a word, to acquire the pure LuAG polycrystalline nanoparticles, the reaction time is suggested to be >3 h.

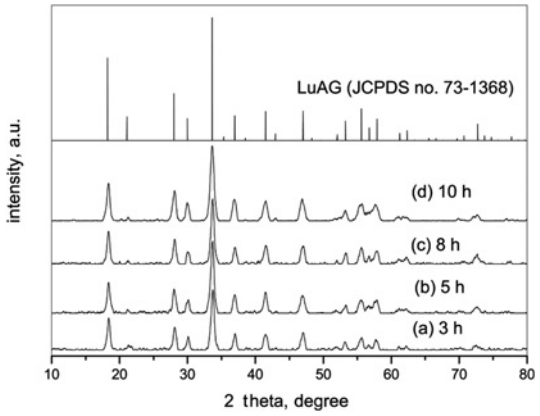

Fig. 5 *XRD patterns of as-synthesised products in en solution at 220°C using different reaction times*

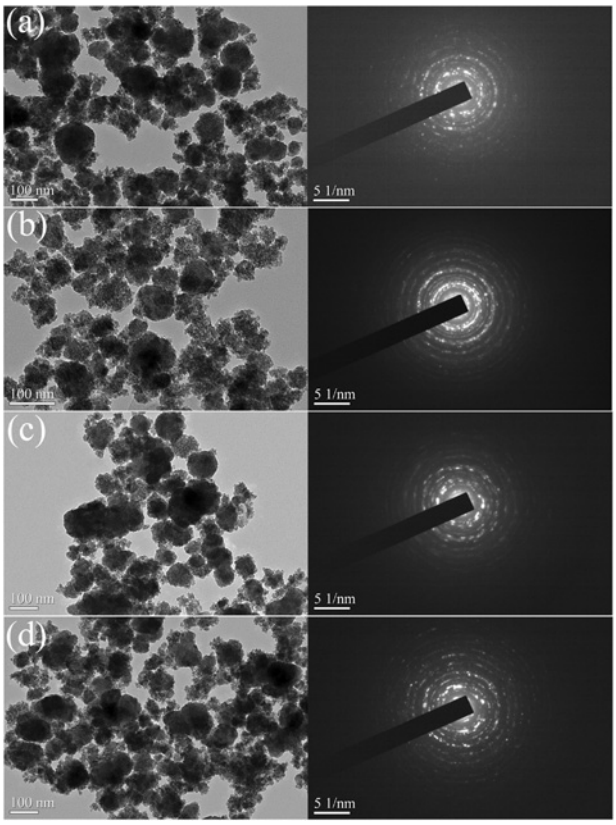

Fig. 6 *TEM micrographs and SAED patterns of as-prepared particles in en solution at 220°C using different reaction time*
a 3 h
b 5 h
c 8 h
d 10 h

3.4. Influence of dispersant: In this Letter, citric acid is used as a dispersant to decrease the particle size and increase dispersion of the nanoparticles. Figs. 7 and 8 reveal XRD patterns and TEM micrographs of the particles obtained before and after citric acid addition, respectively. As can be seen from Fig. 7, a pure-phase LuAG is obtained and no other crystalline phases are detected before and after citric acid addition. The SAED patterns (Fig. 8) further verify the presence of well-crystallised LuAG structures. Furthermore, it can also be seen from Fig. 8 that the as-obtained nanoparticles before citric acid addition show spherical-like

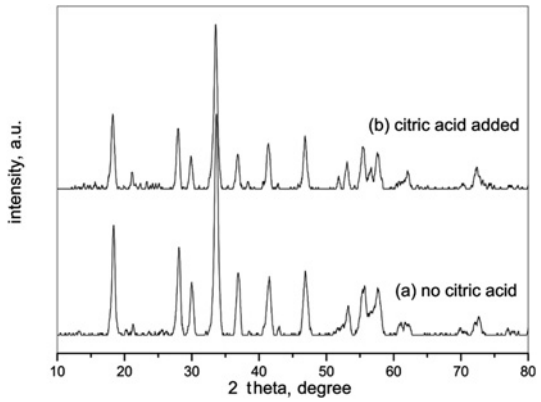

Fig. 7 *XRD spectra of the particles obtained before and after citric acid addition*

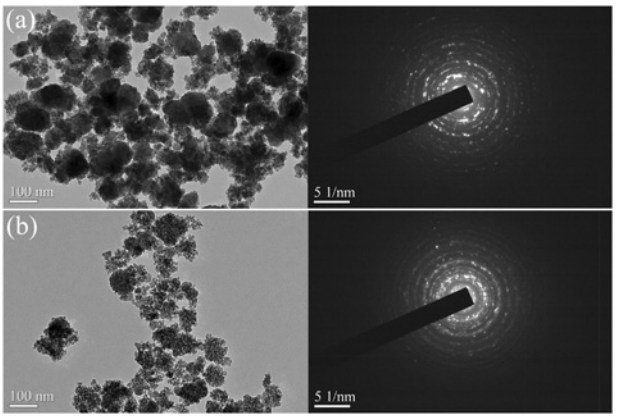

Fig. 8 *TEM micrographs and SAED patterns of the nanoparticles obtained before and after citric acid addition*
a No citric acid
b Citric acid added

structures and have serious agglomeration, while citric acid addition effectively prevents the agglomeration of powders, and leads to smaller particle size and more uniform dispersion.

4. Conclusion: A simple one-step synthesis of LuAG nanoparticles by a solvothermal method is presented. XRD and FTIR patterns show when the reaction solvent is en, the reaction temperature is $\not<200°C$ and the reaction time is >3 h, the pure LuAG nanoparticles can be obtained. The TEM micrographs and SAED patterns show the as-prepared LuAG nanoparticles are well-crystallised and quasi-spherical shape with a particle size of around 100 nm. The addition of citric acid as a dispersing agent decreases particle size and increases dispersion of nanocrystallines. This one-step solvothermal method at low temperatures offers a novel route to synthesise LuAG nanoparticles.

5. Acknowledgments: The research was supported by the Key Scientific Research Project in Colleges and Universities of Henan Province (grant no. 15A140045) and the Science and Technology Project of China Textile Industry Association (grant no. 2015020).

6 References

[1] Fan L.C., Xu J., Shi Y., *ET AL.*: 'Effects of hydroxy propyl cellulose (HPC) surfactant on fabrication, microstructure and optical properties of Ce^{3+}:$Lu_3Al_5O_{12}$ (Ce:LuAG) transparent ceramics', *Adv. Powder Technol.*, 2016, **27**, (2), pp. 610–617

[2] Xing L., Peng L.M., Gu M., *ET AL.*: 'Solvothermal synthesis of lutetium aluminum garnet nanopowders: determination of the optimum synthesis conditions', *J. Alloys Compd.*, 2010, **491**, (1), pp. 599–604

[3] Xing L., Xu X.B., Gu M., *ET AL.*: 'Dielectric relaxations in undoped, Ce-doped and Ce,Zr-codoped Lu3Al5O12 single crystals', *J. Phys. Chem. Solids*, 2009, **70**, (3–4), pp. 595–599

[4] Nakatsuka A., Yoshiasa A., Yamanaka T.: 'Cation distribution and crystal chemistry of $Y_3Al_{5-x}Ga_xO_{12}$ ($0 \leq x \leq 5$) garnet solid solutions', *Acta. Crystallogr. B*, 1999, **55**, (3), pp. 266–272

[5] Xing L., Peng L.M.: 'Comparison of preparation and formation mechanism of LuAG nanopowders using two different methods', *Micro Nano Lett.*, 2012, **7**, (6), pp. 529–532

[6] Wu Y.T., Zhang G.Q., Ren G.H.: 'Band-gap engineering in $Lu_3Al_5O_{12}$:Pr by Sc^{3+} or In^{3+} substitution', *J. Lumin.*, 2014, **145**, (1), pp. 371–378

[7] Feng L., Wang Z.B., Cao C., *ET AL.*: 'Warm-white persistent luminescence of $Lu_3Al_2Ga_3O_{12}$:Pr^{3+}', *J. Rare Earths*, 2017, **35**, (1), pp. 47–52

[8] Chen S.Y., Fan J.T., Pan L.J., *ET AL.*: 'Synthesis of Yb:$Lu_3Al_5O_{12}$ nano powders with the reverse strike co-precipitation method: influence of decomposition of NH_4HCO_3', *J. Rare Earths*, 2016, **34**, (9), pp. 901–907

[9] Uhlich D., Huppertz P., Wiechert D.U., *ET AL.*: 'Preparation and characterization of nanoscale lutetium aluminium garnet (LuAG) powders doped by Eu^{3+}', *Opt. Mater.*, 2007, **29**, (11), pp. 1505–1509

[10] Boukerika A., Guerbous L.: 'Investigation of the structural and photoluminescence properties of Ce^{3+}-doped LuAG nanopowders prepared via sol–gel method', *Opt. Mater.*, 2015, **40**, pp. 14–19

[11] Dubnikova N., Garskaite E., Beganskiene A., *ET AL.*: 'Sol–gel synthesis and characterization of sub-microsized lanthanide (Ho, Tm, Yb, Lu) aluminium garnets', *Opt. Mater.*, 2011, **33**, (8), pp. 1179–1184

[12] Xing L., Qu L.H., He Q., *ET AL.*: 'Solvothermal fabrication and luminescent properties of nanoLuAG:Ce phosphors', *Micro Nano Lett.*, 2014, **9**, (1), pp. 60–63

[13] Zhang X.D., Xu G.G., Wang J.Y., *ET AL.*: 'Synthesis of YAG by the solvothermal method', *Rare Metal Mater. Eng.*, 2007, **36**, (S1), pp. 128–130

[14] Li X., Liu H., Wang J.Y., *ET AL.*: 'Rapid synthesis of YAG nano-sized powders by a novel method', *Mater. Lett.*, 2004, **58**, (19), pp. 2377–2380

[15] Wu Z.G., Zhang X.D., He W., *ET AL.*: 'Solvothermal synthesis of spherical YAG powders via different precipitants', *J. Alloys Compd.*, 2009, **472**, (1), pp. 576–580

doi: 10.1049/mnl.2017.0316